Malaysian Journal of Chemistry, 2023, Vol. 25(3), 232-243
(Special Issue: *Rubbercon2022*)

Hydration of Hardened Cement Paste Incorporates Nano-Palm Oil Fuel Ash at Later Age: The Microstructure Studies

Mohd Azrul Abdul Rajak[1*], Zaiton Abdul Majid[2] and Mohammad Ismail[3]
[1]Preparatory Centre for Science and Technology, Universiti Malaysia Sabah, Jln. UMS, 88400 Kota Kinabalu Sabah, Malaysia
[2]Department of Chemistry, Faculty of Science, Universiti Teknologi Malaysia, Johor Bahru, Johor, Malaysia
[3]School of Civil Engineering, Faculty of Engineering, Universiti Teknologi Malaysia, Johor Bahru Johor, Malaysia
*****Corresponding author (e-mail: azrulrajak88@ums.edu.my)

Cement replacement using pozzolanic materials in nano-sized particles could improve the mechanical and durability of concrete. A study on the hydration of cement in hardened cement paste (HCP) could assist the investigation of nano-POFA (nPOFA) as a potential supplementary cementing material (SCM). Hence, the present work aims to examine the hydration of HCP incorporates nPOFA and the pozzolanic activity of nPOFA in cement matrix through the microstructure studies. A set of nPOFA-HCP were prepared with a cement replacement in range of 10-60% and the paste were cured for 90 days. The microstructural investigation of nPOFA-HCP was conducted via X-Ray diffraction (XRD) analysis, Field Emission Scanning Electron Microscope (FESEM) analysis, Thermogravimetric (TG) analysis and Fourier Transfrom Infrared (FTIR) spectroscopy analysis. The diffractogram show the calcium hydroxide (CH) peak at at 2θ = 18.1º and 34.0º in 30nPOFA and 40nPOFA HCP is low compare than other pastes. The 30nPOFA and 40nPOFA give a low value of the relative loss weight of CH at later age through the TG analysis. Meanwhile, the morphology study display 30nPOFA and 40nPOFA HCP possess a dense and compact microstructure. FTIR analysis study the peaks of O-H symmetric stretching, C-O asymmetric stretching, Si-O asymmetric stretching and C-O bending stretching. Overall, the findings reveals the presence of nPOFA in cement matrix enhance the microstructure of cement matrix through the acceleration of cement hydration and the pozzolanic reaction. The cement replacement up to 40% with nPOFA could give an optimum result to produce a better cement-based products.

Keywords: Nona-palm oil fuel ash (nPOFA); pozzolanic activity; hardened cement paste; cement hydration

Received: January 2023; Accepted: February 2023

Ordinary Portland Cement (OPC) is a conventional construction material worldwide. The hydration of OPC in water results in the formation of cementitious binding material and other byproducts (see Equation 1), which contribute to the mechanical properties and durability of cement-based products [1]. Nonetheless, the industrial production of OPC increased the greenhouse effect due to high carbon dioxide emissions and high energy consumption during the cement manufacturing process [2,3]. Furthermore, over a long period of time, the continuous quarry of natural raw materials to produce cement will eventually bring about the minimization of natural sources [3].

In response to these concerns and other related environmental issues, supplementary cementing materials (SCM) are now regarded as a viable alternative to cement for reducing cement consumption. Presently, industrial and agricultural by-products such as ash fly ash, ground granulated blast-furnace slag (GGBFS), silica fume, palm oil fuel ash (POFA), rice husk ash (RHA), and sugar cane bagasse ash are gaining global attention [3–5]. These materials provide a satisfactory result in improving the mechanical properties and durability of concrete [3,4].

In this study, POFA has been used to be as SCM. POFA is a by-product from the combustion process of palm oil biomass at high temperatures for the electricity supply process in a mill. POFA is a silica-rich material that could generate secondary calcium silicate hydrate (CSH) gel through the pozzolanic reaction as can be seen in Equation 2 to Equation 5 [6,7].

$$2(3CaO.SiO_2)\ (s) + 6H_2O\ (l) \rightarrow 3CaO.2SiO_2.3H_2O\ (s) + 3Ca(OH)_2(s) \quad \text{[Eq. 1][1]}$$

Cement notation

$$2C_3S + 6H \rightarrow 3CSH + 3CH$$

Alite + Water → Calcium silicate Hydrate gel + Calcium Hydroxide

†Paper presented at Rubbercon2022

$$SiO_2\,(s) + 2H_2O\,(l) \rightleftharpoons H_4SiO_4\,(aq) \quad \text{[Eq. 2]}$$

$$H_4SiO_4\,(aq) + OH^-(aq) \rightleftharpoons H_3SiO_4^-\,(aq) + H_2O(l) \quad \text{[Eq. 3]}$$

$$H_3SiO_4^-\,(aq) + OH^-(aq) \rightleftharpoons H_2SiO_4^{2-}(aq) + H_2O(l) \quad \text{[Eq. 4]}$$

$$Ca^{2+}\,(aq) + H_2SiO_4^{2-}\,(aq) + H_2O\,(l) \rightarrow CaO.SiO_2.2H_2O\,(s) \quad \text{[Eq. 5]}$$

Previous studies have shown that POFA enhances mechanical properties and durability performance, including mechanical strength, tensile strength, drying shrinkage, and heat of hydration [6,7]. This contribution is due to POFA's ability to act as a filler, as nucleation sites of CSH and supply additional CSH through the generation of secondary CSH from the pozzolanic reaction, which resulted in the enhancement of microstructure hardened cementitious matrix [6,7].

Because of the promising revolutionary changes in the physical and chemical properties of various downstream products, the application of nanotechnology has attracted global attention in construction fields [8,9]. Nano-materials as additives and SCM in cement matrix research have grown rapidly in recent years due to their high potential as construction materials when compared to conventional materials. In comparison to conventional SCM, literature on using nanosized-SCM in cementitious matrix revealed the ability to improve fresh and hardened properties as well as the durability of concrete and mortar [8,9].

Yet, the utilization of nano-sized (nPOFA) as SCM is still in a limited number of studies especially those focuses on the microstructure study of hardened cement paste (HCP) at later ages [10–14]. Therefore, the present study aim to investigate the progress of cement hydration and pozzolanic reaction of HCP incorporates nPOFA at 90 days of curing ages through the microstructure study. The qualitative and quantitative analysis of nPOFA HCP were examined through microstructure study via thermal analysis, X-Ray diffraction (XRD) analysis, Fourier Transform Infrared (FTIR) analysis, morphological analysis. The strength activity index (SAI) was conducted through the preparation of nPOFA mortars to confirm the microstructure analysis.

EXPERIMENTAL

Preparation of Nano Sized Palm Oil Fuel Ash

Raw POFA were collected from the local palm oil mill in Johor, Malaysia. POFA were dried dan all large and foreign substances were removed through sieving process. The nano-sized of POFA were obtained through the grinding process of POFA using modified Los Angeles Abrasion test machine in 6 h and followed with ceramic mall milling in 30 h with a 10:1 weight ratio of the balls to powder. The chemical composition and physical properties of OPC and nPOFA were shown in Table 1. In accordance with ASTM C618-12a [15], nPOFA is categorized in Class C pozzolan since the sum of silica, aluminium oxide and iron oxide are within minimum requirement of 50%. In addition, sulphur oxide in nPOFA is less than 5% and the amount of calcium oxide is higher than 10%.

The particle size analysis of nPOFA was analyzed via Transmission electron microscopy (TEM) analysis and was shown in Fig. 1. Based on TEM analysis, the particle size distribution of nPOFA was illustrated in Fig. 2. It is shows that the particle size distribution of nPOFA is found to in range of 20 to 90 nm.

Table 1. Chemical composition and physical properties of nPOFA and OPC.

Component	SiO_2	CaO	Al_2O_3	Fe_2O_3	MgO	SO_3	LOI	S_{BET} (m^2/g)	True Density (g/mL)	Passing 45 µm sieve (%)
OPC	21.45	60.98	3.62	4.89	1.22	2.30	1.37	-	-	-
nPOFA	54.8	14.0	7.24	4.47	4.14	0.71	8.5	145.35	1.71	100

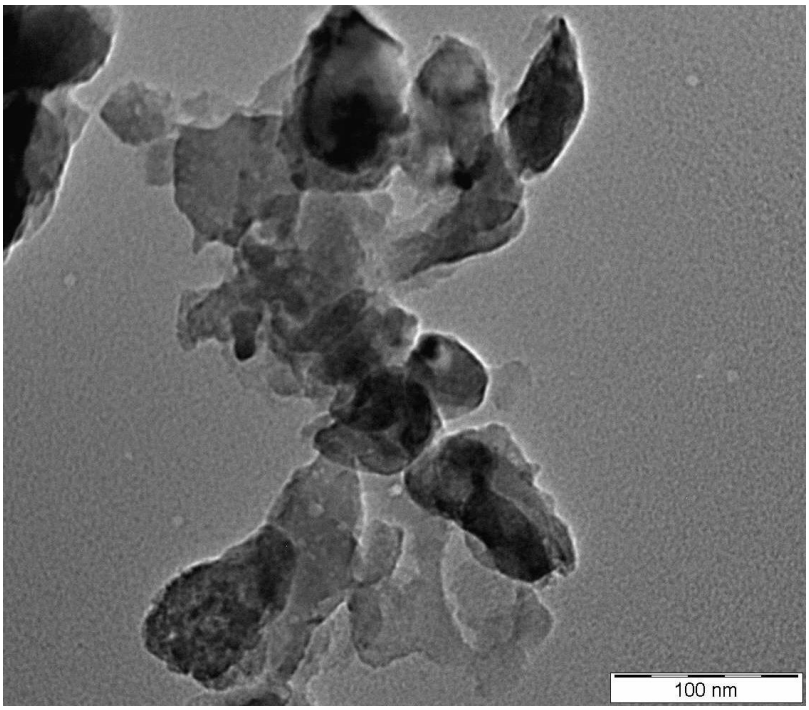

Figure 1. TEM analysis of nPOFA.

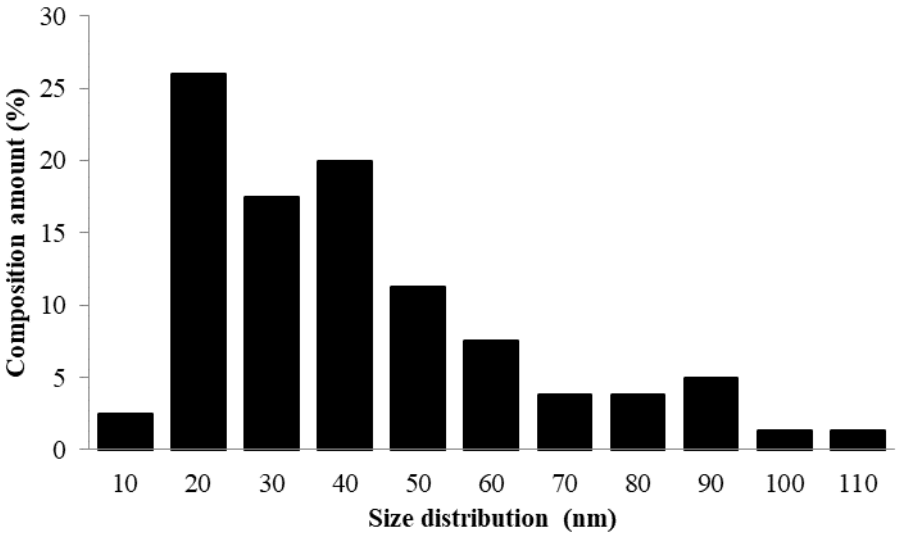

Figure 2. Particle distribution size of nPOFA.

Preparation of Hardened Cement Paste

Cement paste cubes were prepared by incorporating nPOFA ranging from 10% w/w to 60% w/w. The OPC paste was used as a control paste and was prepared with a water to cement ratio of 0.28, whereas the nPOFA cement paste was prepared with a constant water to binder ratio of 0.35 [16]. Mix designs for the six cubes of cement paste specimens are shown in Table 2. The cement paste was prepared in accordance with the procedures outlined in ASTM C109/C109M [17]. The paste was cast in cubic moulds 50 mm × 50 mm × 50 mm. The cement paste-filled moulds were covered with a damp cloth for 24 h before curing in a saturated lime solution at 23±2ºC for 90 days.

Table 2. Mix designs of cement paste of OPC and nPOFA.

Specimen	Cement (g)	nPOFA (g)	Water/ binder
Control OPC	600	0	0.28
10%nPOFA	540	60	0.35
20%nPOFA	480	120	0.35
30%nPOFA	420	180	0.35
40%nPOFA	360	240	0.35
50%nPOFA	300	300	0.35
60%nPOFA	240	360	0.35

Microstructure Analysis of Hardened Cement Paste

The hydration of hardened cement paste (HCP) was monitored at 90 days curing age through the micro-structure analysis. The (HCP) cubes were crushed manually and immersed in acetone for 3 days to remove the existence of water in hardened cementitious matrix, as it necessary in arresting the hydration [18]. The HCP specimens were then put in an oven at a temperature of 50 ± 5ºC for 24 h to allow the evaporation of the remaining acetone. Determination of the relative amount of calcium hydroxide ($Ca(OH)_2$) were performed through thermal analysis via Perkin-Elmer Thermal Pyris Diamond TG/DTA analyzer. XRD analysis were executed using Siemens/ Bruker Advance D5000 diffraction with Cu K_α radiation (λ = 1.54060 Å) to monitor the progress of hydration through the intensity of peaks conforming to the alite (C_3S), belite (C_2S) and $Ca(OH)_2$. Measurements were taken from $2\theta = 7^o$ to 70^o using a step size and scan speed of 0.05^o and 0.05^o min^{-1}, respectively. The FTIR spectrometer (Perkin Elmer Spectrum) was used to record FTIR spectra ranging 4000 to 450 cm^{-1} in Nujol mull and as KBr pellet. Morphology analysis of HCP was studied by scanning electron microscopy (SEM), which was performed on a Phenom ProX SEM, operated at 10 kV.

Compressive Strength Test of Mortar

The preparation of OPC mortars and nPOFA mortars were conducted in accordance with [17]. The detailed mix design is shown in Table 3. The mass ratio of sand to binder was fixed at 2.75 for all mortar mixes. The fresh mortar paste was casted in 50 mm x 50mm x 50 mm cubic moulds. The cubic mortars were demoulded after 24 h casting and placed in the saturation lime water at temperature of 23 ± 1ºC until its test age.

Compressive strength test was executed triplicate for each mortar specimens in accordance to ASTM C109/C109M-12 [17] using ELE International ADR 2000 hydraulic press with a capacity of 2000 N. The percentage of strength activity index (SAI) of mortars was calculated in compliance with ASTM C311-11b [19].

RESULTS AND DISCUSSION

The hydration progress of cement paste incorporates nPOFA at later age (90 days curing age) was monitored through the microstructure analysis includes thermal analysis, XRD analysis, FTIR analysis and morphology analysis. The mechanical strength of mortars is based on the SAI value and to confirm microstructure study.

Table 3. Mix design for OPC and nPOFA mortars.

Specimen	Cement (g)	nPOFA (g)	Sand (g)	$\frac{\text{Water}}{\text{Cement + nPOFA}}$
OPC	500	-	1375	0.48
10nPOFA	450	50	1375	0.66
20nPOFA	400	100	1375	0.66
30nPOFA	350	150	1375	0.67
40nPOFA	300	200	1375	0.68
50nPOFA	250	250	1375	0.69
60nPOFA	200	300	1375	0.69

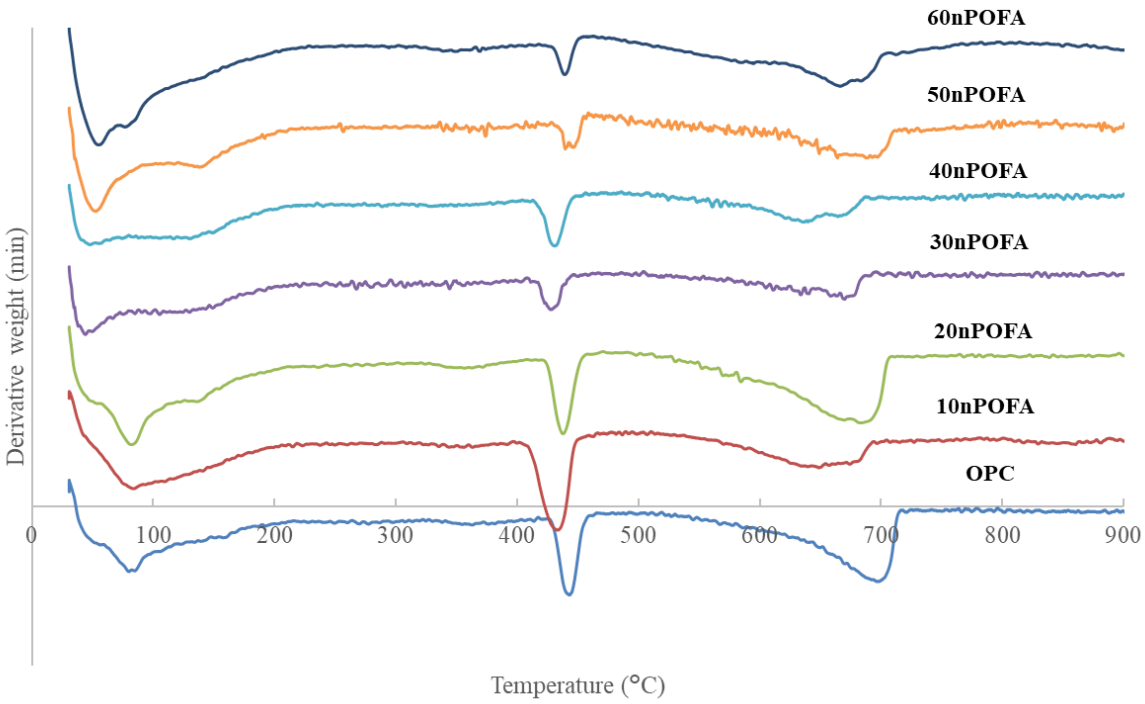

Figure 3. DTG curves of cement paste at 90 days curing age.

Thermal Analysis

Figure 3 shows the DTG curves of nPOFA and OPC HCP at 90 days curing ages. Three significant weight losses were detected from DTG curves of all nPOFA and OPC HCP, which include:

i. First endotherm peak in the temperature range 30ºC to 210ºC could attributed to the decomposition of the evaporated water;

ii. Second endotherm peak in the temperature range between 410ºC to 480ºC corresponds to the dihydroxylation of $Ca(OH)_2$ and;

iii. Third endotherm peak in the temperature range 510 °C to 700 °C could attributed to the decarbonation of carbonated phase.

Previous research indicates that the assessment of $Ca(OH)_2$ weight loss percentage based on thermal analysis were used in explaining the degree of cement hydration and pozzolanic reaction since $Ca(OH)_2$ is a major hydrated product. Equation 6 depicts the dexydroxylation of $Ca(OH)_2$.

Therefore, the rate of cement hydration and pozzolanic reaction of nPOFA HPC were discussed based on the relative weight loss of $Ca(OH)_2$ which indicate the content of $Ca(OH)_2$ in HCP. The relative weight loss of $Ca(OH)_2$ as shown in Fig. 4. As shown in Fig. 4, OPC have a high $Ca(OH)_2$, 4.9 %, when compared to all nPOFA HCP. Meanwhile, 30nPOFA HCP has the lowest relative weight loss in $Ca(OH)_2$, at 1.9 %. The increase in nPOFA replacement in cement matrix from 10% to 30% contributes to a decrease in $Ca(OH)_2$ content from 10% to 30% in HCP.

The pozzolanic reaction progress at later ages can explain the differences value in $Ca(OH)_2$ content between OPC and nPOFA HCP, as shown in Equation 2 to Equation 5. Pozzolanic reactions used $Ca(OH)_2$, a byproduct of cement hydration, to react with silica from nPOFA to generate secondary CSH. In this case, 30-40% w/w nPOFA replacement in cement blended could result in better performance in cement-nPOFA based products due to the high activity of the pozzolanic reaction to produce secondary CSH, which could improve mechanical strength.

$$\underset{\text{Portlandite/ calcium hydroxide}}{Ca(OH)_2} \xrightarrow{410\text{-}480^{o}C} \underset{\text{Calcium oxide}}{CaO + H_2O} \qquad \text{[Eq. 6]}$$

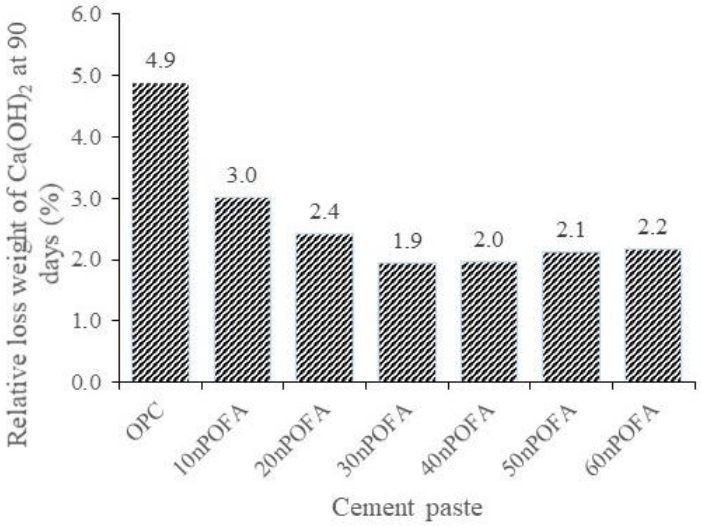

Figure 4. Relative loss of $Ca(OH)_2$ phase obtained from thermogram of OPC and nPOFA HPC at 90 days curing age/.

Table 4. Assignment of peaks on 2-Theta values of XRD.

Minerals	Abbreviation	2-Theta	ICDD files
Alite	C_3S	29.4, 30.1, 51.7	42-551
Portlandite	$Ca(OH)_2$	18.1, 34.1, 47.2	33-302
Tobermorite	CSH	29.2	34-0002
α-Quartz	-	26.5	64-6312

Minerology Analysis

Qualitative analysis of hydration progress OPC and nPOFA HCP was conducted through mineralogy analysis based on the significant peaks on 2-theta values of XRD as can be seen in Table 4.

Fig. 5 shows the diffractogram of OPC and nPOFA HPC at 90 days of curing age. The intensity peak at 2θ = 29.4º to 30.1º is assigned to the overlap peaks of alite and CSH. The peaks at 2θ = 51.7º also confirm the existence of alite. Other intense peaks at 2θ = 18.1º, 34.1º and 47.2º are observed in all HCP are assigned to Portlandite. The presence of α-Quartz was detected in all nPOFA HCP based on the appearance of a peak at 2θ = 26.5º.

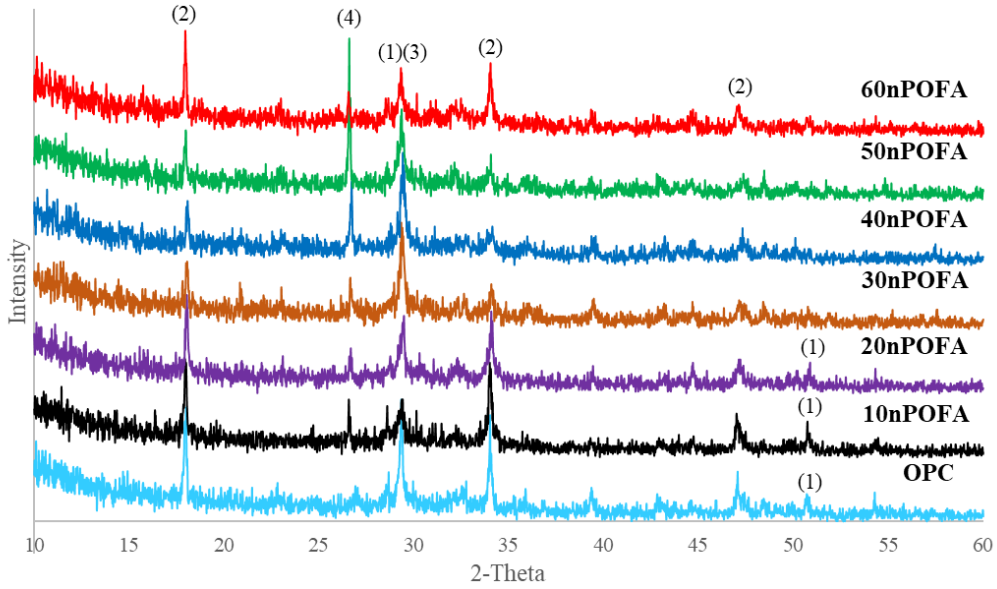

Figure 5. Diffractogram of OPC and nPOFA HCP at 9 days curing age.
Notation- (1) Alite, (2) Portlandite, (3) CSH, (4) α-Quartz

The result suggests that the low intensity peaks of Portlandite at 30nPOFA and 40nPOFA HCP compared to OPC HCP due to the pozzolanic reaction progress that occurs in the cement matrix (see Equation 2 to Equation 5). It is confirmed by the reduction peaks of alite (peaks at $2\theta = 51.7^{o}$) for 30nPOFA and 40nPOFA. As the peak intensity of alite reduces, the peaks of Portlandite increase. However, the reduction of intensity peaks of Portlandite in nPOFA HCP especially in 30nPOFA and 40nPOFA HCP could explain a high rate of pozzolanic reaction in the HCP to reduce the amount of Portlandite. The mineralogy analysis confirms the result in a relative loss of $Ca(OH)_2$ through thermal analysis. The low relative loss of $Ca(OH)_2$ in the nPOFA HCP with 30% w/w and 40% w/w replacement of nPOFA could give an optimal performance to reduce $Ca(OH)_2$.

Fourier Transform Infrared Analysis

The FTIR spectrum of OPC and nPOFA HPC at 90 days of curing age is shown in Fig. 6. Meanwhile, Table 5 shows the detection absorption bands from FTIR spectrum for each OPC and nPOFA HPC. The sharp peaks in the range 959.3 cm^{-1} to 969.2 cm^{-1} is assigned to the Si-O asymmetric stretching vibration, which corresponds to the polymerization of silicate unit (SiO_4^{4-}) as its outcome from the formation of CSH gel during the cement hydration. The medium strong peak around 3650 cm^{-1} is assigned to the O-H is symmetric stretching vibration which arises from the generation of Portlandite. The appearance of broad peak in the range of 3377 to 3500 cm^{-1} is assigned to the asymmetric and symmetric stretching vibration of O-H from water molecule that come from water-cement system of hydration process. Meanwhile the peak in the range of 1620 to 1660 cm^{-1} represent the O-H bending vibration, originated from the water molecule incorporates in the hydration of cement. The peak with strong intensity1450 cm^{-1} and 875 cm^{-1} are the characteristic bands for C-O stretching vibration and C-O bending vibration, respectively. The peaks correspond to the carbonate (CO_3^{-}) group, produced from the carbonation of CH with carbon dioxide to produce calcite.

The infrared spectroscopy analysis could examine qualitatively the hydration progress and pozzolanic reaction in HCP incorporates nPOFA based on the presence of the peak Si-O asymmetry stretching vibration as it reflects the CSH formation. According to Table 5, the frequency of Si-O for 30nPOFA HCP display a progressive shift to a higher frequency compared to OPC HPC. This could be attributed to the high formation of silicate group (CSH) during the hydration of cement [20]. It is suggested, the replacement of 30% w/w of nPOFA in cement could give a high rate of pozzolanic reaction in the cement matrix. It was further confirmed by the decrease intensity of C-O peak around 1450 cm^{-1} as the replacement of nPOFA in cement increase. It is suggested the reduction of of $Ca(OH)_2$ due to the high rate of pozzolanic reaction to consume $Ca(OH)_2$ to produce secondary CSH. (see Equation 2 to Equation 5). The result is confirmed by the findings in thermal analysis.

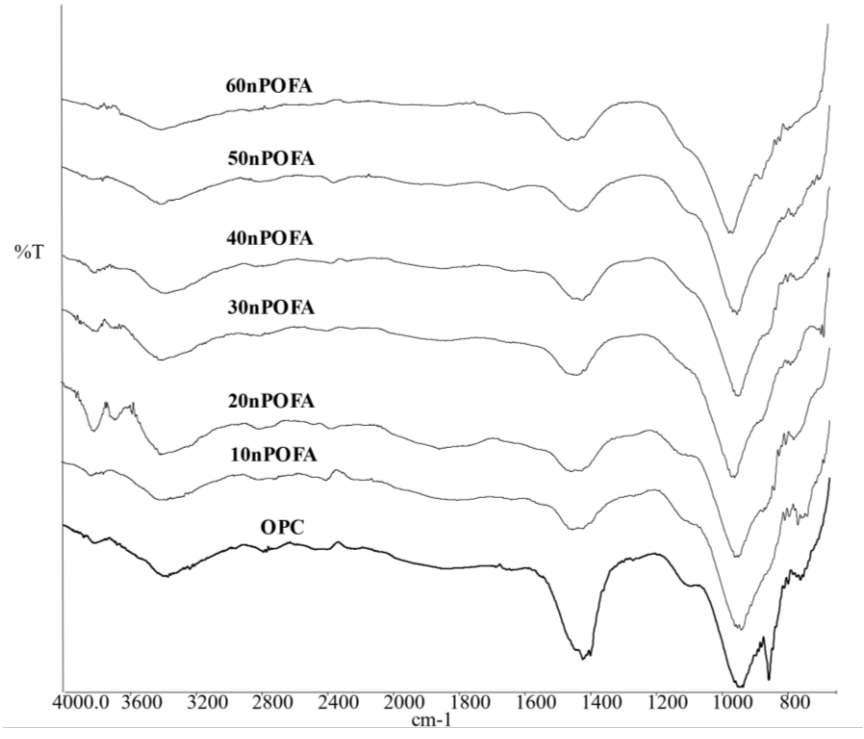

Figure 6. FTIR spectrum of OPC and nPOFA HCP at 90 days curing age.

Table 5. Wavenumbers of peaks from FTIR analysis for OPC and nPOFA HCP at 90 days curing age.

	Assignment peak							
Cement paste	**O-H (CH)**	**O-H**		**C-O**		**Si-O**	**S-O**	
OPC	3674.1	3377.0	1620.3	1433.0	874.0	965.2	1113.9	-
10nPOFA	-	3412.7	1620.2	1468.7	883.9	959.3	1086.1	
20nPOFA	3670.6	3404.76	1640.11	1466.7	881.9	961.2	1125.8	-
30nPOFA	3674.6	3400.8	1623.21	1439.0	874.0	969.2	1173.9	689.6
40nPOFA	-	3388.9	1637.6	1435.0	874.0	965.2	1107.9	-
50nPOFA	3638..9	3396.8	1655.1	1435.0	880.0	959.3	1074.2	-
60nPOFA	3634.92	3460.0	1649.1	1456.1	876.0	959.3	1167.91	-

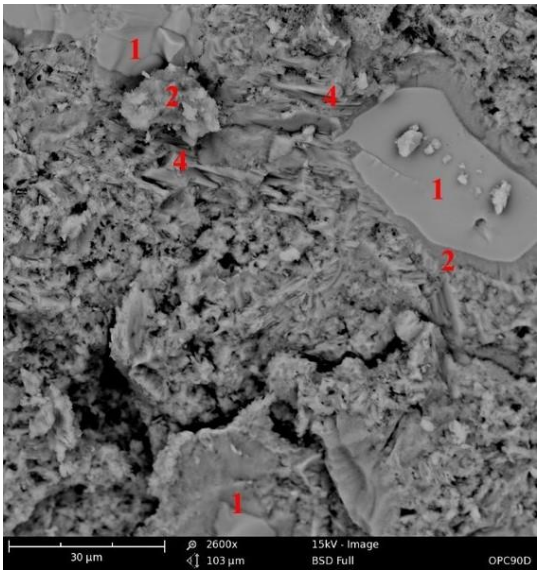

Figure 7. SEM micrograph of OPC paste at 90 days of curing age.

Morphological Characteristics Hardened Cement Paste

The morphological of nPOFA HCP examined the hydration progress of anhydrous cement and the pozzolanic reaction of nPOFA. Fig. 7 shows the morphology image of OPC paste at 90 days of curing age. It is observed the presence of anhydrous alite, CSH and hexagonal plates of $Ca(OH)_2$ crystals resulting a high homogenous mixture of paste. The fibrous gel of CSH formation is observed at the surface of anhydrous alite or coated the $Ca(OH)_2$ crystals. However, the appearance of pores also detected in the image that suggest the hydration of cement in OPC paste not completely produce the dense and compact microstructure. At later age of OPC paste, the strength durability is based on the products of cement hydration.

The nPOFA HCP morphology at 90 days curing age is shown in Fig. 8. As can be seen in Fig. 8, the microstructure of nPOFA HCP at later age is denser and compact compared to OPC paste. Obviously the 30nPOFA and 40nPOFA HCP at this curing age possesses high dense and compact microstructure. It can be seen, the microstructure for both HCP contributed by the anhydrous alite, CSH from hydration of cement, the secondary CSH from pozzolanic reaction and $Ca(OH)_2$ crystals. Similar findings were observed by the other researchers as they claimed that the hcp at later age produced more CSH and the secondary CSH, resulting in a denser and compact microstructure [8,9]. Meanwhile, the 50nPOFA and 60nPOFA HCP show the microstructure with high voids and least homogeneous microstructure. The unreacted nPOFA also observed in 50nPOFA and 60nPOFA HCP. This observation also similar with previous study where the unreacted nPOFA were detected at mortar with high replacement of nPOFA at late age [11].

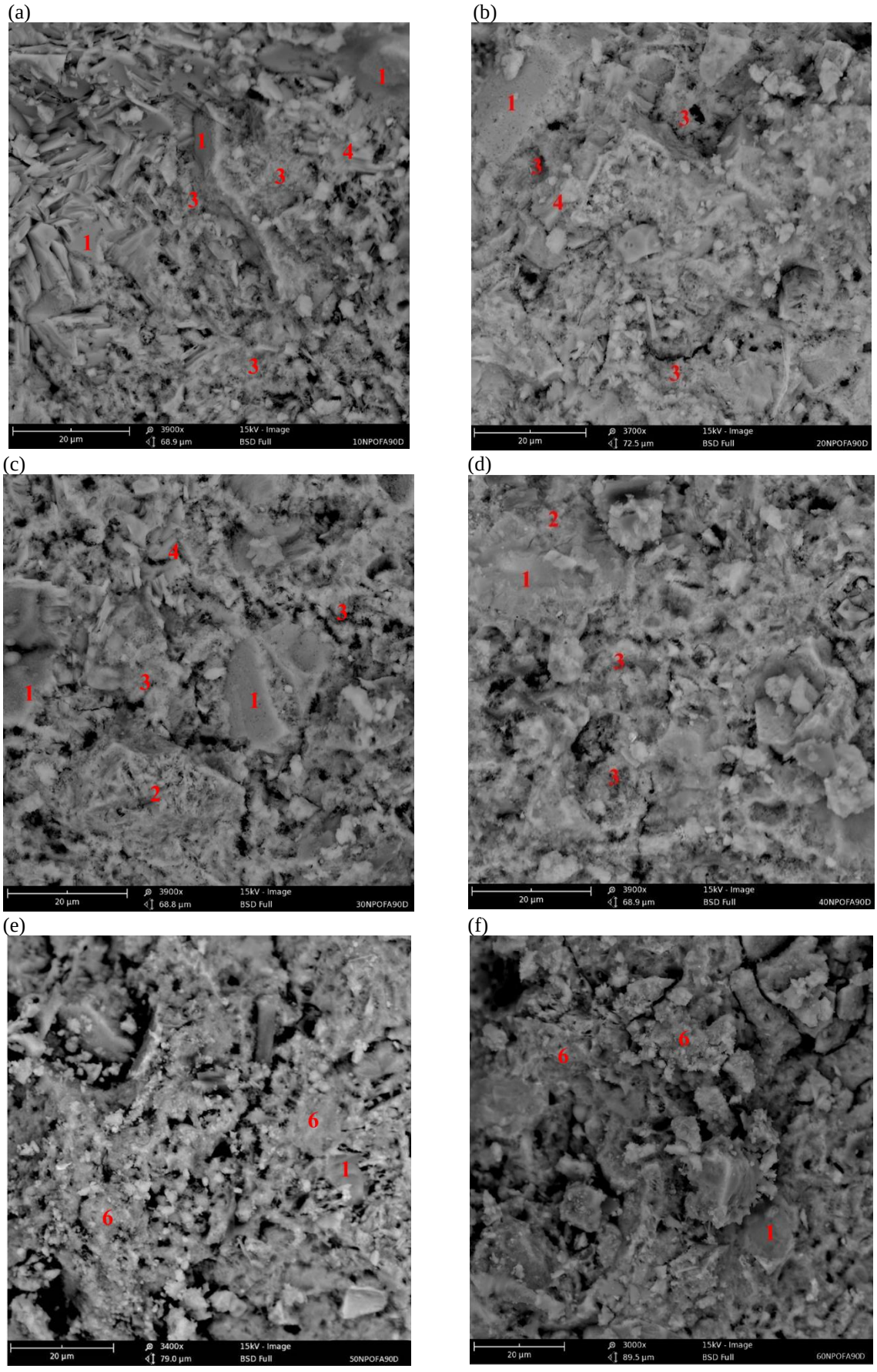

Figure 8. SEM micrographs of (a) 10nPOFA (b) 20nPOFA, (c) 30nPOFA (d) 40nPOFA (e) 50nPOFA and (f) 60nPOFA HCP at 90 days of curing age. Notation: 1- Alite, 2- CSH 3- Secondary CSH 4- $Ca(OH)_2$, 5- Ettringite 6- Unreacted nPOFA.

It is suggested that the homogeneous hardened cementitious matrix in nPOFA hcp at 90 days curing age could be attributed to the enhancement of microstructure by the high formation CSH (hydrated products) and the secondary CSH (pozzolanic reaction product). The $Ca(OH)_2$ crystals in this curing age lost its hexagonal shape reflects the dissolution of $Ca(OH)_2$ in cement matrix to react with nPOFA particles to generate secondary CSH. It is suggested, the visible fibrous CSH gels nucleates on the surface of $Ca(OH)_2$ crystals is the products from pozzolanic reaction [10]. The high fineness of nPOFA particles increase the distribution of on the cement matrix as it increases the ability of nPOFA to act as nucleation sites and filler. Lim et. al [21] and Samadi et. al [22] also claim the similar agreement where nPOFA is a better filler due to the high fineness of its particle as it can access and fill up the pore structure of HCP. As result, a high dense and compact microstructure of HCP is obtained. In addition, the high specific surface area of nPOFA particles accelerates the cement hydration, while its small diameter particles increase the dissolution of silica in the pores solution [11]. The morphological analysis suggests that the development of OPC paste is dependent on CSH (cement hydration), while the hardened cementitious matrix in nPOFA HCP was contributed by the formation of both CSH (cement hydration) and the secondary CSH (pozzolanic reaction). Meanwhile, the presence of nPOFA particles in the blended cement enhances the hardened cementitious matrix into a dense and compact microstructure.

Strength Activity Index of Mortars

For a substance to be accepted as a SCM, the mortars incorporate SCM must achieve 75% of SAI value as requirement by ASTM C618-12a [15]. In this test, the OPC mortars are the control specimen. Table 6 shows the SAI of OPC and nPOFA mortars. As can be seen in Table 6, the 30nPOFA mortars have the highest SAI value amongst the nPOFA mortars, 108.2% respectively. It can be observed that all the mortars at this curing age exceed the SAI of OPC mortars except for 50nPOFA and 60nPOFA mortars.

In nPOFA mortars, the replacement with 30% w/w of nPOFA demonstrates the highest mortar strength, while the cement replacement with 60% nPOFA shows the lowest mortar strength. It is suggested that the increasing SAI value from 10% w/w to 40% w/w replacement could be attributed to the high rate of pozzolanic reaction of nPOFA in the mortar matrix to generate a sufficient secondary CSH to increase the strength of mortar. The previous literature also claimed that the high fineness increases the replacement in cement as it provides the high pozzolanic reaction in the cement matrix [8,9]. The results was confirmed by the microstructure analysis, 30nPOFA and 40nPOFA HCP shows the high $Ca(OH)_2$ consumption (see Figure 4), whereby the dense and compact microstructures with less amount of $Ca(OH)_2$ crystals and empty voids were observed in the 30nPOFA and 40nPOFA HCP (see Figure 7). Meanwhile, it is suggested the low strength of 50nPOFA and 60nPOFA mortars could be attributed to the reduction of cement amount (dilution effect) and retardation effects. The presence of high amount of SCM in the blended cement retards the hydration of anhydrous cement and increase the water consistency in the blended cement.

Table 6. Strength activity index (SAI) of OPC and nPOFA mortars.

Mortar	Water / Cement + nPOFA	Flow	90 Days	Mean– *SAI (%)*
OPC	0.44	111	54.305 54.853 52.051	52.117 - *100*
10nPOFA	0.66	108	54.982 56.395 54.602	55.326 – *106.2*
20nPOFA	0.66	110.5	54.614 56.317 55.953	55.628 – *106.7*
30nPOFA	0.67	109	58.543 54.88 55.738	56.387 – *108.2*
40nPOFA	0.68	107	54.323 55.711 54.719	54.918 – *105.4*
50nPOFA	0.69	110.5	49.336 48.694 47.031	48.354 – *92.8*
60nPOFA	0.69	112	45.303 47.197 46.519	46.340 – *88.9*

The high specific surface area of nPOFA particle increase its distribution in the hardened cementitious matrix, as its small diameter of particles increase the dissolution of both crystalline and amorphous silica, resulting the high pozzolanic reactivity of nPOFA. As results, the rapid pozzolanic reaction occurs in the nPOFA mortars to produce high secondary CSH, which form a high dense and compact microstructure of hardened mortars. These agreements were similar to the previous studies [10,11] as they authors claimed that the increasing of SCM fineness into nanosized particles improve its pozzolanic reactivity and enhance the strength of cement-based products.

Based on these findings, the replacement of cement with 30% nPOFA gives the highest SAI value compared to the other amount of replacement. However, while the replacement of cement up to 40% nPOFA in blended cement gives the lower SAI compared to 30nPOFA mortar, its SAI value exceeded the SAI of the control mortar specimen. Hence it is suggested to consider the replacement of cement up to 40% nPOFA.

CONCLUSION

In summary, the progress of cement hydration and pozzolanic reaction at later age of HCP can be conducted quantitative and qualitative analysis through microstructure study. The results show 30% w/w of nPOFA replacement in cement matrix could give a better microstructure property of the cement-based product. However, it can be considered to substitute the cement up to 40% w/w nPOFA replacement since the strength of 40nPOFA mortar is higher than the OPC mortar at 90 days curing age.

ACKNOWLEDGEMENTS

The authors thank to the staff of Department of Chemistry, Faculty of Science and Department of Structure and Materials, School of Civil Engineering, Faculty of Engineering, Universiti Teknologi Malaysia. The authors also acknowledge the Universiti Malaysia Sabah dan Ministry of High Education Malaysia for the financial aid.

REFERENCES

1. Beaudoin, J. and Odler, I. (2019) Hydration, setting and hardening of Portland cement in *Lea's Chemistry of Cement and Concrete, 5th ed., Elsevier Ltd.*

2. del Strother, P. (2019) Manufacture of Portland cement in *Lea's Chemistry of Cement and Concrete, 5th ed., Elsevier Ltd.*

3. Ndahirwa, D., Zmamou, H., Lenormand, H. and N. Leblanc (2022) The role of supplementary cementitious materials in hydration, durability and shrinkage of cement-based materials, their environmental and economic benefits: A review. *Cleaner Materials*, **5**, 100123.

4. Rahla, K. M., Mateus, R. and Bragança, L. (2019) Comparative sustainability assessment of binary blended concretes using Supplementary Cementitious Materials (SCMs) and Ordinary Portland Cement (OPC). *Journal of Clean Production*, **220**, 445–459.

5. Gudainiyan, J. and Kishore, K. (2022) A review on cement concrete strength incorporated with agricultural waste. *Materials Today: Proceedings in 3rd Biennial International Conference on Future Learning Aspects of Mechanical Engineering 2022*.

6. Hamada, H. M., Thomas, B. S., Yahaya, F. M., Muthusamy, K., Yang, J., Abdalla, J. A. and Hawileh, R. A. (2021) Sustainable use of palm oil fuel ash as a supplementary cementitious material: A comprehensive review. *Journal of Building Engineering*, **40**, 102286.

7. Aisheh, Y. I. A. (2023) Palm oil fuel ash as a sustainable supplementary cementitious material for concrete: A state-of-the-art review. *Case Studies in Construction Materials*, **18**, e01770.

8. Monteiro, H., Moura, B. and Soares, N. (2022) Advancements in nano-enabled cement and concrete: Innovative properties and environmental implications. *Journal of Building Engineering*, **56**, 104736.

9. Abdalla, J. A., Thomas, B. S., Hawileh, R. A. and Syed Ahmed Kabeer K. I. (2022) Influence of nanomaterials on the workability and compressive strength of cement-based concrete. *Material Today: Proceedings*, **65**, 2073–2076.

10. Rajak, M. A. A., Majid, Z. A. and Ismail, M. (2015) Morphological characteristics of hardened cement pastes incorporating nano-palm oil fuel ash. *Procedia Manufacturing*, **2**, 512–518.

11. Wi, K., Lee, H. S., Lim, S., Song, H., Hussin, M. W. and Ismail, M. A. (2018) Use of an agricultural by-product, nano sized palm oil fuel ash as a supplementary cementitious material. *Construction and Building Material*, **183**, 139–149.

12. Wi, K., Wang, K., Han, J., Lee, H. S. and Lim, S. (2022) Effects of nano palm oil fuel ash on hydration of cement under the accelerated carbonation curing. *Materials Letter*, **327**, 132935.

13. Rajak, M. A. A., Majid, Z. A. and Ismail, M. (2019) Cement hydration extents for hardened cement paste incorporating nanosized-palm oil

fuel ash: A thermal and XRD analysis study in *Lecture Notes in Civil Engineering - ICACE 2019*. *Springer Nature Singapore Pte Ltd*, 61–70.

14. Rajak, M. A. A., Majid, Z. A. and Ismail, M. (2019) Pozzolanic activity of nanosized palm oil fuel ash: A comparative assessment with various fineness of palm oil fuel ash. *IOP Conference Series: Earth and Environment Science*, **220**, 012061.

15. ASTM C618-12a (2017) Standard specification for coal fly ash and raw or calcined natural pozzolan for use in concrete. *American Society for Testing and Materials*, C0618-12.

16. Bentz, D. P. and Stutzman, P. E. (2006) Curing, hydration, and microstructure of cement paste. *ACI: Materials Journal*, **103(5)**, 348–356.

17. ASTM C109/C109M-12 (2013) Standard test method for compressive strength of hydraulic cement mortars (Using 2-in . or [50-mm] cube specimens), American Society for Testing and Materials C0109_C0109M-12.

18. Zhang, J. and Scherer, G. W. (2011) Comparison of methods for arresting hydration of cement. *Cement and Concrete Research*, **41(10)**, 1024–1036.

19. ASTM C311-11b (2013) Standard test methods for sampling and testing fly ash or natural pozzolans for use in portland-cement concrete. *American Society for Testing and Materials*, C0311-11B.

20. Bhat, P. A. and Debnath, N. C. (2011) Theoretical and experimental study of structures and properties of cement paste: The nanostructural aspects of CSH. *Journal of Physics and Chemistry of Solids*, **72**, 920–933.

21. Lim, N. H. A. S., Ismail, M. A., Lee, H. S., Hussin, M. W., Sam, A. R. M. and Samadi, M. (2015) The effects of high volume nano palm oil fuel ash on microstructure properties and hydration temperature of mortar. *Construction and Building Materials*, **93**, 29–34.

22. Samadi, M., Huseien, G. F., Lim, N. H. A. S., Mohammadhosseini, H., Alyousef, R., Mirza, J. and Rahman, A. B. A. (2020) Enhanced performance of nano-palm oil ash-based green mortar against environment. *Journal of Building Engineering*, **32**, 101640, 1–13.